Journal of Medicinal Chemistry

Article

pubs.acs.org/jmc

Exploring the Binding Sites of Glycogen Synthase Kinase 3. Identification and Characterization of Allosteric Modulation Cavities

Valle Palomo,[†] Ignacio Soteras,[†] Daniel I. Perez, Concepción Perez, Carmen Gil, Nuria Eugenia Campillo, and Ana Martinez*

Instituto de Quimica Medica-CSIC, Juan de la Cierva 3, 28006 Madrid, Spain

ABSTRACT: Glycogen synthase kinase 3 (GSK-3) is an important drug target for human severe unmet diseases. Discovery and/or design of allosteric kinase modulators are gaining importance in this field not only for the increased selectivity of this kind of compounds but also for the subtle modulation of the target. This last point is of utmost importance for the GSK-3 inhibition as a therapeutic approach. GSK-3 activity is completely necessary for life, and only the aberrant overactivity found in the pathologies should be inhibited with its inhibitors treatment. We performed here a search for the druggable sites on the enzyme using the fpocket algorithm with the aim to provide allosteric potential binding sites on it and new clues for further drug discoveries. Moreover, our results allowed us to determine the binding sites of different GSK-3 ATP noncompetitive inhibitors, such as manzamine A and the new small molecule VP 0.7, providing evidence for potential allosteric inhibition of GSK-3.

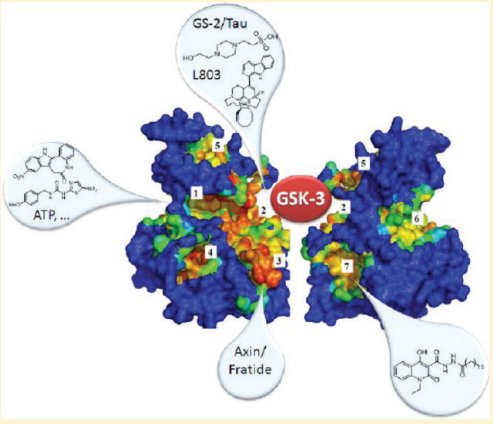

INTRODUCTION

Glycogen synthase kinase 3 (GSK-3) is a well-known protein kinase involved in the last step of glycogen synthesis. However, in this century, GSK-3 has emerged as a fascinating drug target for human severe unmet diseases, such as diabetes type II, bipolar disorders, chronic inflammatory diseases, and neurodegenerative pathologies.[1,2] Moreover, some of its inhibitors have demonstrated efficacy in different animal models, which opens a successful future for their pharmaceutical development and a hope for a new generation of efficient therapies.[3]

In Alzheimer's disease (AD), an overactivity and/or overexpression of GSK-3 plays a central role in the pathology linking all the neuropathological hallmarks described for this devastating disorder, such as amyloid deposition, tau hyperphosphorylation, gliosis, and neuronal death.[4] In fact, the thiadiazolidindione (TDZD) derivative called Tideglusib, an ATP noncompetitive GSK-3 inhibitor, has recently finished a pivotal phase II clinical trial in 20 mild to moderate AD patients. Disclosed results showed not only safety and tolerability for the drug but also a trend in the enhancement of cognition abilities in patients.[5] Furthermore, Tideglusib has been recognized by the Food and Drug Administration (FDA) and European Medicines Agency (EMA) as an orphan drug for the treatment of a rare tauopathy called progressive supranuclear palsy, with its phase II clinical trial ongoing.

The lack of effective therapies for neurodegenerative diseases, and especially for AD, which is the most common form of dementia among the elderly population, leads us to consider the search for new and specific GSK-3 inhibitors as a relevant task in current medicinal chemistry research.[6,7]

There are many compounds with different scaffolds able to inhibit GSK-3 in an ATP competitive manner, which sometimes should offer adverse secondary effects in a potential chronic treatment.[8,9] The human kinome has more than 500 protein kinases that share a high degree of identity in the catalytic site, the ATP binding pocket, with the kinase selectivity being one of the main challenges in the search and design of protein kinase inhibitors.[10] One of the possibilities to gain kinase selectivity is the discovery of allosteric modulators.[11] These compounds generally act by inducing conformational changes on the enzyme modulating the kinase activity without competing with ATP for binding to the catalytic domain. Allosteric modulators of protein kinases are likely to be more selective, since they bind to unique regions of the kinase and may be useful in overcoming resistance developed to drugs which compete with ATP.[12] Furthermore, they provide more subtle modulation of kinase activity than simply blocking ATP entrance. This point is of utmost importance for GSK-3 modulation as a therapeutic approach for the treatment of human illnesses because its inhibitors, as new drugs, should only inhibit the aberrant GSK-3 kinase activity implicated in a variety of human diseases.[13]

There are different chemical families of organic compounds reported in the literature that do not compete with ATP in their GSK-3 inhibition, and different binding modes to the enzyme have been described (Figure 1). The first reported family was the small heterocyclic TDZD family.[14] Although their mechanism of action is not experimentally confirmed yet,

Received: July 26, 2011
Published: November 3, 2011

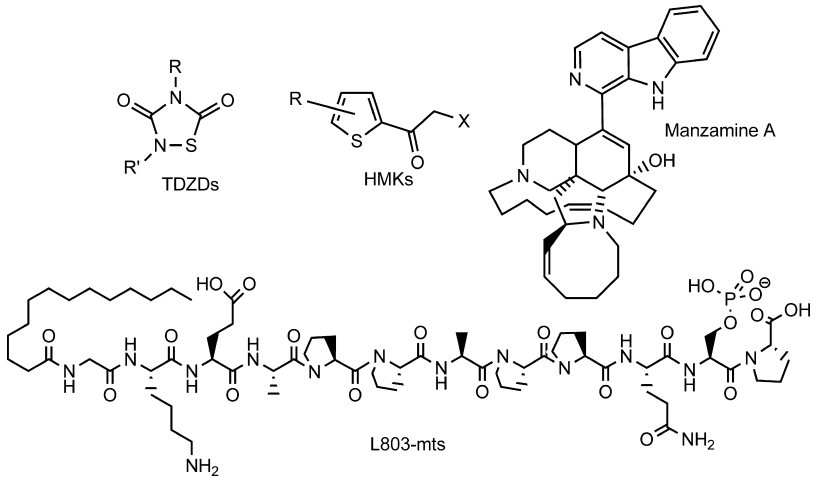

Figure 1. ATP noncompetitive GSK-3 inhibitors.

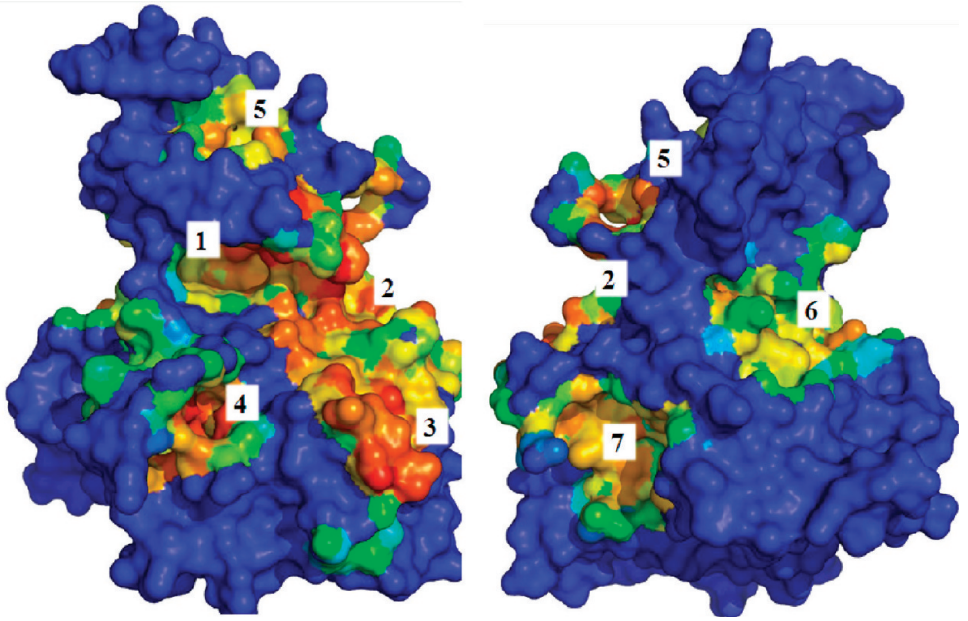

Figure 2. Cavities found by hpocket. These seven cavities match with those found by fpocket in the 25 PDB structures analyzed independently.

Table 1. Number of Pockets Found on Different GSK-3 Structures

PDB structures	1GNG	3GB2	1O9U, 1Q4L, 1Q5K, 1Q3D, 3L1S	205K, 20W3, 3DU8, 3F7Z, 3F88, 3I4B, 3M1S, 3PUP	1I09, 1J1B, 1J1C, 1PYX, 1Q41, 2JLD	1H8F, 1Q3W, 1R0E	1UV5
no. of pockets found	7	9	10	11	12	13	17

it is postulated to play a possible role in the modification of a cysteine key residue found in the active site of GSK-3.[15] The second family of compounds known was the halomethylketone (HMK) derivatives[16] which have been recently described as the first irreversible inhibitors of this enzyme.[17] In this case, inactivation of the enzyme is due to the formation of an irreversible covalent sulfur−carbon bond between the key Cys199 located at the entrance of the ATP site of GSK-3 and the HMK moiety.[18] Different peptides have also been described as modulators of GSK-3 activity.[19] On one hand, protein−protein interaction is interfered with different endogenous peptides. Thus, Axin and Fratide peptides bind to GSK-3 and disrupt the low affinity homodimer that this kinase forms.[20] From the therapeutic point of view, more relevant are the small peptides designed as substrate competitive GSK-3 inhibitors.[21] Although the most advanced candidate L803-mts has shown efficacy in different animal models of neurological diseases,[22] the low pharmacokinetic profile associated with the peptidic chemical scaffold prevents its complete development to clinical trials. Finally, it is worth mentioning the fact that the alkaloid called manzamine A, isolated from sponges, has been recently described as a cell-permeable GSK-3 inhibitor with no ATP competition, being able to decrease tau phosphorylation in cell cultures,[23,24] and recently molecular modeling studies revealed a potential allosteric site on GSK-3 for it.[25]

The main goal of this work is to discover druggable binding sites on GSK-3 able to be modulated by small-molecule interactions. We have used fpocket to analyze the overall kinase

dx.doi.org/10.1021/jm200996g | J. Med. Chem. 2011, 54, 8461–8470

surface, validating our results with some of the GSK-3 inhibitors known until now. Moreover, we here described a new chemically diverse small molecule found in our laboratory as a new hit for allosteric inhibitors of GSK-3.

RESULTS AND DISCUSSION

Surface Cavities Determination. Detection, comparison, and analyses of ligand binding pockets are pivotal to structure-based drug design endeavors[26] and can help in identifying binding pockets or allosteric sites to start the design of small-molecule ligands with therapeutic effects. There are a lot of programs with this aim, and they can be classified according to the type of algorithm used. There are mainly two types of algorithms: evolutionary and structure-based algorithms. The second category can be subdivided into geometry- and energy-based algorithms.[27] The last ones compute the interactions of a solvent molecule on the protein surface in order to detect the local surface properties of a cavity. The most popular examples of geometry-based algorithms are potential active sites with spheres. On the other hand, the strategy followed by the evolutive algorithms is completely different. They operate by looking for proteins with similar sequences; then fragments of conserved residues are identified in order to look for the key ones which are relevant for the protein function and potentially targeted by new future drugs.

Here, we have used the free geometry-based algorithm fpocket (http://fpocket.sourceforge.net),[28] to study the GSK-3 surface with the aim to identify allosteric binding sites, since allostery represents one of the most common and powerful means to regulate protein function.

The fpocket software core can be resumed by three major steps.[29] During the first step, the whole ensemble of alpha spheres, a sphere that contacts four atoms on its boundary and contains no internal atom, is determined from the protein structure. Fpocket returns a prefiltered collection of spheres. The second step consists in identifying clusters of spheres close together, identifying pockets, and removing clusters of poor interest. The final step calculates properties from the atoms of the pocket, in order to score each pocket.

Prior to testing the fpocket skills, a search of tridimensional structures of GSK-3 from the Protein Data Bank (PDB) was carried out. Twenty-five different GSK-3-ligand complexes obtained by X-ray diffraction with a resolution better than 2.5 Å were available at the moment of this study in the Protein Data Bank (PDB). All of them were considered for the calculation of cavities for ligand binding sites. The 25 GSK-3/ligand structures were processed similarly, removing water molecules, inhibitors, cofactors, and metal ions (even those from the catalytic site), and leaving only the monomer protein fragment. Moreover, as the results derived from fpocket are slightly dependent on the starting orientation, some of the structures randomly selected were rotated.

The different cavities found by fpocket on different structures of GSK-3 are shown in Table 1. The program identified in the majority of structures used between 10 and 12 different cavities. At least 7 pockets were always found in every structure used in the calculation, and in one of them, fpocket could identify up to 17 different cavities. The results given by the program were sorted in a list ranked using a score based on a knowledge-based SiteScore.[27] We have analyzed seven well conserved binding sites along the different GSK-3 structures used.

Analysis of Potential Binding Sites. Careful inspection of the results allowed pinpointing several facts. We found some highly reproducible cavities that appear in most of the GSK-3 structures analyzed, and others that appear randomly in fewer structures. Some of these areas were sometimes detected as two different cavities and others as a joint cavity. Taking all these facts into account, we constructed a table with the more representative pockets (nos. 1−7), which were present in the great majority of the GSK-3-ligand complex structures. When fpocket found the same cavity as two different ones in a given structure, it has been annotated as two numbers in the table. In Table 2 is presented the score given by the program to cavities (nos. 1−7) in each PDB structure.

Table 2. Principal Pockets Found on GSK-3β[a]

	principal pockets found on GSK-3β (1−7)[b]						
PDB code	1	2	3	4	5	6	7
1GNG	2	n.f.	4, 11	3	10	n.f.	1
1H8F	1, 8	1	n.f.	3	5	4	2, 9
1I09	1, 3	1, 11	n.f.	2	7	8	4, 6
1J1B	1	10	2	4	6, 9	11	3, 5, 8
1J1C	1	n.f.	8	2	5	6	4, 7, 11
1O9U	5, 8	7	4	3	n.f.	n.f.	1, 2
1PYX	1	1, 7	n.f.	3	13	12	2, 4
1Q3D	1	10	8	2	4	7	3, 5
1Q3W	3, 4	3, 8	n.f.	1	5	10	2, 11
1Q41	1	12	11	2	6	8	3, 4
1Q4L	2	4	10	3	7	5	1
1Q5K	1	1	9	3	n.f.	8	2, 5
1R0E	1	10	8, 12	2	6	9	3, 4
1UV5	1	9, 13	12	2	8	5, 7	4, 3
2JLD	1	n.f.	11	2	7, 8	10	4, 3
205K	1, 7	9	n.f.	2	n.f.	5	4, 3
20W3	1	11	3	2	6	4	5
3DU8	1	n.f.	4	3	5	10	2, 7
3F7Z	1	6	n.f.	2	9	8	3, 5, 7, 4
3F88	2, 11	4, 7	n.f.	1	6	10	3, 5
3GB2	2	n.f.	n.f.	1, 5	4	n.f.	3, 6, 7
3I4B	1	1	5, 6	2	4	n.f.	3
3L1S	1	8, 10	n.f.	3	6	5	2, 4
3M1S	1	5	n.f.	2	n.f.	n.f.	3
3PUP	1	n.f.	5	2	n.f.	n.f.	3
avg score calcd for each pocket	1.9	6.8	7.3	2.4	6.5	7.7	3.8
freq of the corresponding pocket found in GSK-3 structures	25	19	15	25	20	19	25

[a]The numbers relate to the score given by the program fpocket to the cavity in that structure (1 is the best, 12 is the worst). Two or more numbers indicate that this pocket was found as two or more different cavities on the structure. n.f.: not found. [b]See Figure 2.

The variability in the cavities found by fpocket raises the question of the reliability of the predictions. To answer that question, the authors of fpocket developed another application with this purpose: hpocket.[30] This software carries out a BLAST search of similar proteins and outputs a colored coded map of conserved cavities, where the most conserved cavities are shown in red, whereas the less conserved ones are in blue. This kind of analysis must be taken with caution, as a blue area does not mean a region without any cavity; instead, it means an

dx.doi.org/10.1021/jm200996g | J. Med. Chem. 2011, 54, 8461−8470

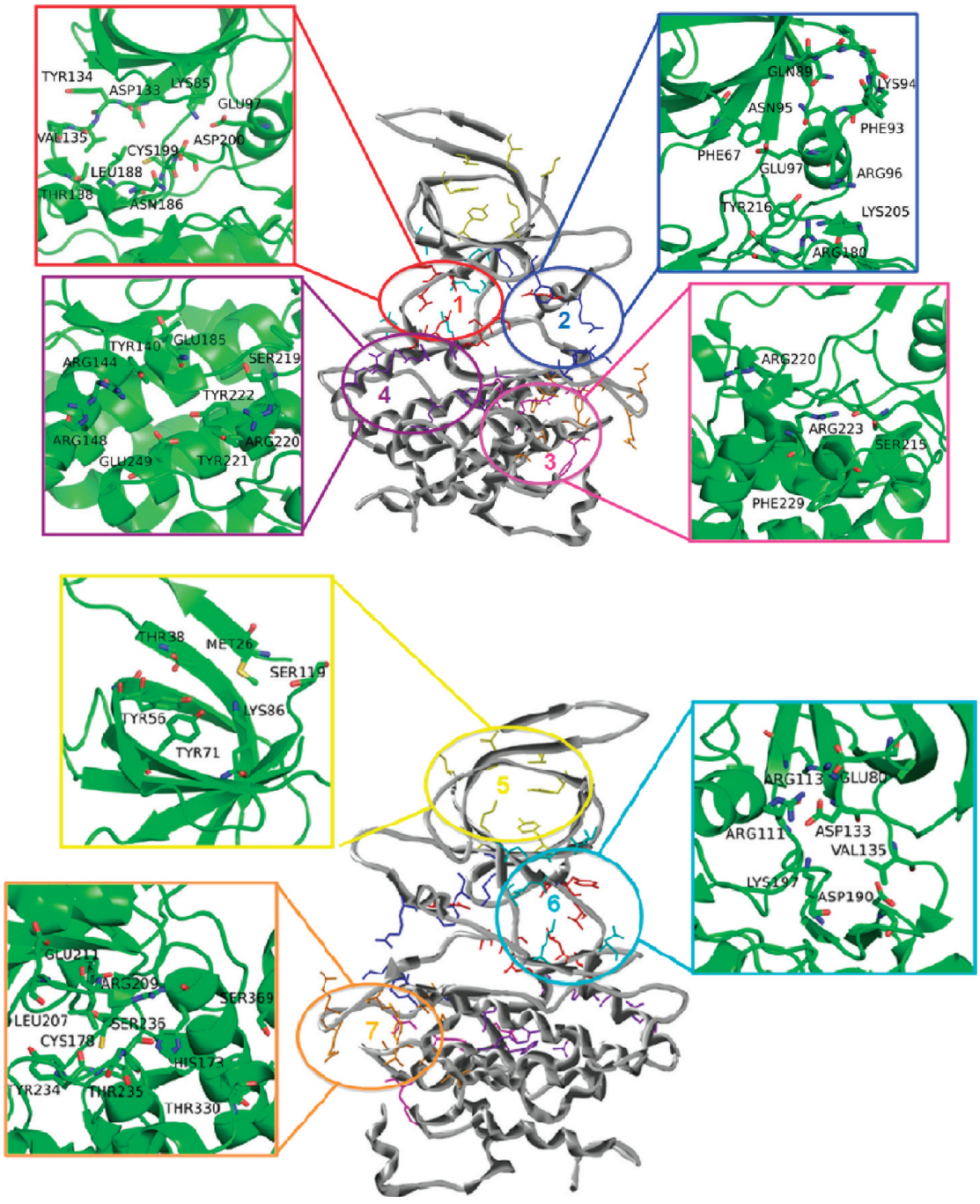

Figure 3. Amino acids involved in each of the seven cavities found on GSK-3. These are as follows: **Cavity 1**, Lys85, Glu97, Asp113, Tyr134, Val135, Thr138, Asn186, Leu188, Cys199, Asp200; **Cavity 2**, Phe67, Gln89, Lys94, Phe93, Asn95, Arg96, Glu97, Arg180, Lys205; **Cavity 3**, Ser215, Arg220, Arg223, Phe229; **Cavity 4**, Tyr140, Arg144, Arg148, Gln185, Ser219, Arg220, Tyr221, Tyr222, Glu249; **Cavity 5**, Met26, Thr38, Tyr56, Tyr71, Lys86, Ser119; **Cavity 6**, Glu80, Arg111, Arg113, Asp133, Val135, Asp190, Lys197; **Cavity 7**, His173, Cys178, Leu207, Arg209, Glu211, Thr235, Ther330, Tyr234, Ser236, Ser369.

area where it is not so common to find a cavity. On the other hand, if a red colored pocket is shown, it means that it is frequently found, so a biological role can be attributed to it. Bearing this in mind, and in order to check the availability of the previous cavities found with fpocket, an hpocket analysis was carried out over one of the structures studied with fpocket.

The result of hpocket was in concordance to our findings with fpocket, as the program could find seven cavities in the same places as we have seen before. In Figure 2 we can see the result given by hpocket with the pockets numbered 1−7.

A detailed description of these seven calculated pockets on GSK-3 has been given. The amino acids involved in each cavity are depicted in Figure 3.

Validation of the Calculated Cavities. From the seven cavities detected in GSK-3 by fpocket to date, only three of them are well-known binding sites on GSK-3, which are ATP-, substrate-, and axin/fratide binding site (cavities 1, 2, and 3, respectively).

The well-known ATP-competitive GSK-3 inhibitors alsterpaullone[31] (IC_{50} = 4 nM) and *N*-(4-methoxybenzyl)-*N*′-(5-

dx.doi.org/10.1021/jm200996g | *J. Med. Chem.* 2011, 54, 8461−8470

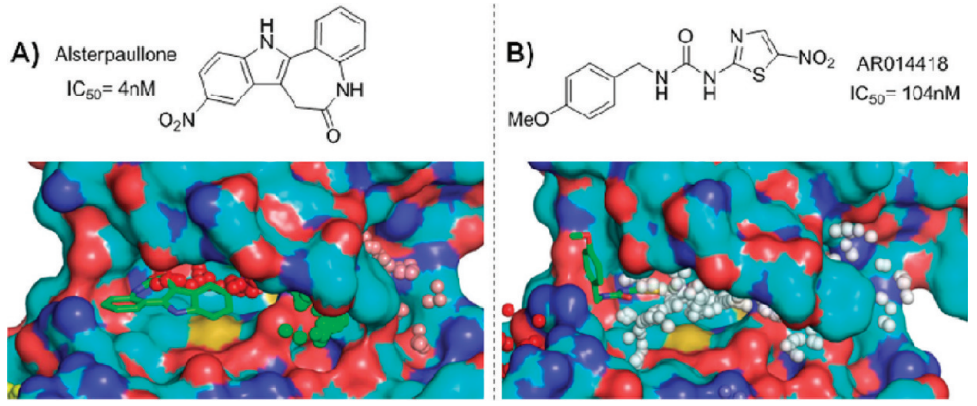

Figure 4. (A) Alsterpaullone inhibitor with 1Q3W structure. (B) AR-A014418 inhibitor with 1Q5K. In these figures we can see how the inhibitors fit in cavity no. 1 determined by fpocket shown by the small colored spheres.

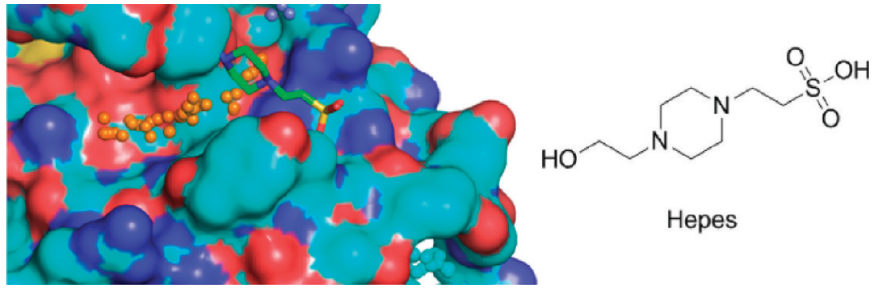

Figure 5. Hepes buffer molecule (green lines) in the 1H8F structure superimposed with the 1UV5 structure and its pockets together with the Hepes 2D-chemical structure.

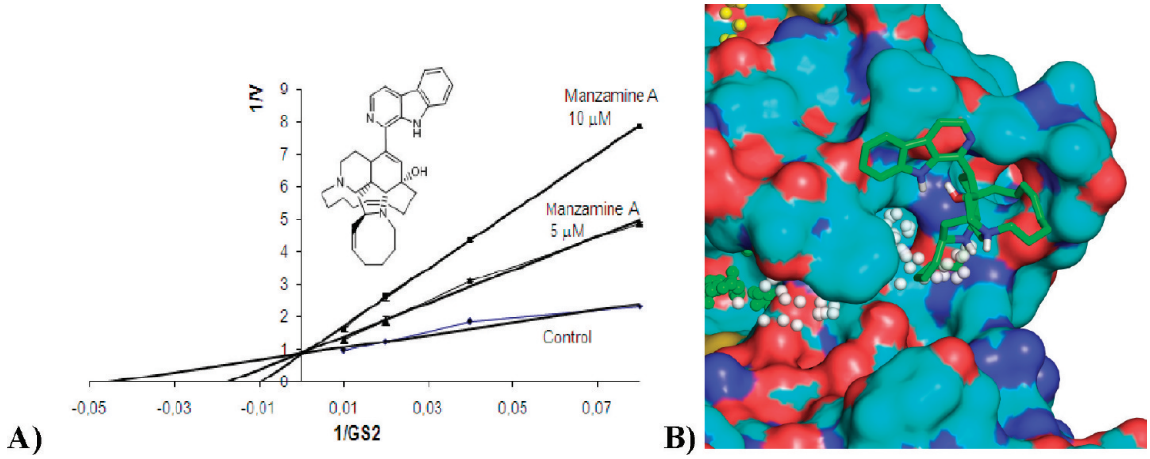

Figure 6. (A) Double-reciprocal plots of kinetic data from assays of GSK-3β activity at different concentrations of manzamine. GS-2 concentrations in the reaction mixture varied from 12.5 to 100 μM. Manzamine concentrations are depicted in the plot, and the concentration of ATP was kept constant at 1 μM. Each point is the mean of two different experiments, each one analyzed in duplicate. (B) Binding site of manzamine A (pocket no. 2, substrate binding site).

nitro-1,3-thiazol-2-yl)urea (AR-A014418)[32] (IC_{50} = 104 nM) were chosen to validate the ATP site, which, as we can see in Figure 2, corresponds to cavity no. 1 found by fpocket. This cavity was found in every PDB structure, and often with low score values, showing a druggable binding site. To see it clearer, we have taken PDB structures 1Q3W and 1Q5K, in which GSK-3 was crystallized with these inhibitors respectively, and placed them together with the result of fpocket for that structure (Figure 4). A good correlation between the experimentally determined binding site and the cavity found with fpocket is found.

Pocket no. 2 was also found in most structures, and this cavity corresponds to the substrate binding site. To validate this result, we have taken the PDB structure 1H8F, in which GSK-3 is crystallized with one molecule of hepes, the buffer used in the process,[33] located in the phosphate recognizing substrate binding site. In Figure 5 we can see how this molecule is placed on cavity no. 2 found by fpocket.

Hamann et al. have postulated by docking studies that derivatives of the ATP noncompetitive inhibitor of GSK-3 manzamine A (Figure 1)[23] bind to the enzyme near the activation pocket formed by three basic residues, Arg96,

dx.doi.org/10.1021/jm200996g | J. Med. Chem. 2011, 54, 8461–8470

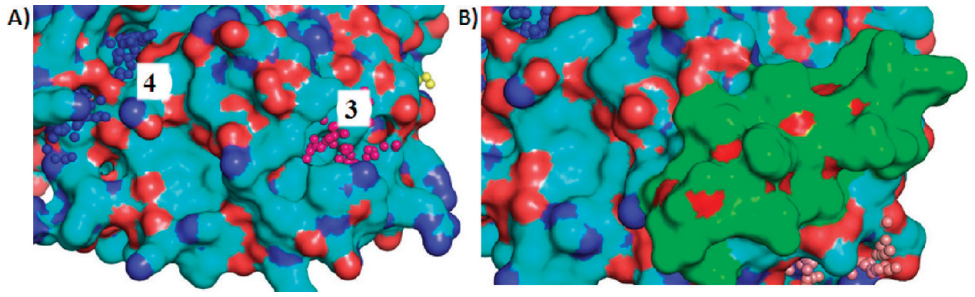

Figure 7. (A) Pocket no. 3 on GSK-3. (B) Axin in the 1O9U structure. This peptide occupies the same location as cavity no. 3.

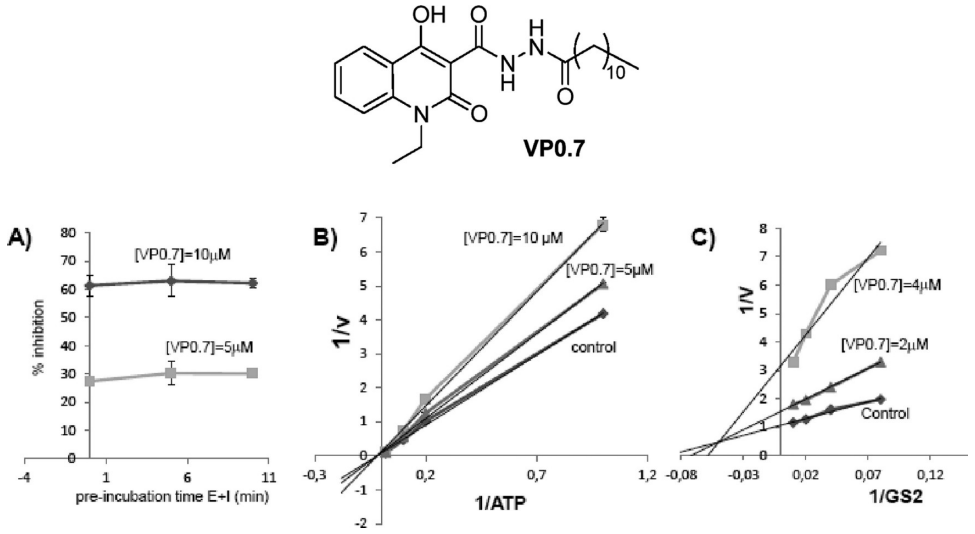

Figure 8. Chemical structure and kinetic data determined for the quinoline derivative VP0.7. (A) Time dependent GSK-3 inhibition of VP0.7. (B) ATP concentrations in the reaction mixture varied from 1 to 50 μM. Compound concentrations are depicted in the plot, and the concentration of GS-2 was kept constant at 12.5 μM. (C) GS-2 concentrations in the reaction mixture varied from 15.5 to 100 μM. VP0.7 concentrations are depicted in the plot, and the concentration of ATP was kept constant at 1 μM. Each point is the mean of two different experiments, each one analyzed in duplicate.

Arg180, and Lys205,[25,34] located in our predicted pocket no. 2. Such predictions had gained support according to recently published studies by Zefirov et al.[35] which confirm this binding site based on a molecular dynamics study. Here, our fpocket calculations are in perfect agreement with the previous results, with our predicted pocket no. 2 being the same as the one reported by both authors.

In this sense, and to check experimentally these theoretical results, we performed competition studies of manzamine A using different concentrations of the peptide GS-2, the GSK-3 substrate used under our experimental conditions. GS-2 is a small peptide similar to skeletal muscle glycogen synthase with the sequence YRRAAVPPSPSLSRHSSPHQ(pS)EDEEE. Double-reciprocal plotting of the data is depicted in Figure 6A. The intercept of the plot in the vertical axis ($1/V$) does not change when the manzamine A concentration increases (from 5 to 10 μM). These kinetic studies would suggest that manzamine A acts as a competitive inhibitor of GS-2 binding. Thus, taking advantage of this data, we placed manzamine A in the site predicted for fpocket (pocket no. 2). Simply, we carried out an optimization of this complex in order to compare it with the results of Hamann, checking in this way the correct prediction of the binding sites with fpocket (Figure 6B).

Moreover, the amino acids involved in pocket no. 2 and depicted in Figure 3 are the same as those recently reported for substrate competitive peptides that inhibit GSK-3.[36] The small peptide L803 has been postulated to interact in an enzyme cavity bordered by the amino acids 89−95 loop,[36] which confirms the results here reported.

The third analyzed pocket (pocket no. 3) was the less common in the 25 GSK-3 structures studied of the 7 here selected, but it has revealed the binding site of the peptides axin and fratide (Figure 7). The scores are high, which indicates a less preferred pocket, perhaps due to exposure of this cavity to the solvent. In this case, we cannot superimpose both structures and perceive the cavity, so we present pocket no. 3 in Figure 7A, and in Figure 7B the peptide axin on GSK-3, as is determined by X-ray diffraction analysis.

After verifying the good correlation between the experimental binding sites and the cavities found with fpocket, we proposed to validate the new binding sites here proposed by docking studies with different structures using the whole molecule of GSK-3. We decided to study *in silico* the binding of a small ligand from our chemical libraries, recently discovered as a reversible GSK-3 inhibitor that does not compete with ATP or with the substrate.

Binding Mode of the Small Molecule VP0.7. As a part of our research program, we have assayed on GSK-3 in vitro activity our in-house chemical library composed by more than 800 diverse chemical structures synthesized in our laboratory during the last 30 years. In this specific screening, we have found that the compound *N*′-dodecanoyl-1-ethyl-4-hydroxy-2-

dx.doi.org/10.1021/jm200996g | *J. Med. Chem.* 2011, 54, 8461−8470

oxo-1,2-dihydroquinoline-3-carbohydrazide (VP0.7) has an IC_{50} value on GSK-3 of 3.01 ± 0.14 μM. Furthermore, the inhibitory activity determined at different preincubation times revealed a reversible inhibition (Figure 8A). Thus, the inhibition of VP0.7 remained unaltered at different preincubation times, mimicking the behavior of known reversible inhibitors. Moreover, kinetic experiments varying both ATP (from 1 to 50 μM) and VP0.7 concentrations (5 and 10 μM), were performed. Double-reciprocal plotting of the data is depicted in Figure 8B. The intercept of the plot in the vertical axis ($1/V$) rises when the VP0.7 concentration increases (from 5 to 10 μM), whereas the intercept in the horizontal axis ($1/[ATP]$) does not change, meaning that, while the enzyme maximal rate (V_{max}) decreases in the presence of the inhibitor, the Michaelis–Menten constant (K_m) remains unaltered. These results would suggest that VP0.7 acts as a noncompetitive inhibitor of ATP binding, because an increase in the ATP concentration (from 1 to 50 μM) does not interfere with enzymatic inhibition. We have also studied the substrate dependence of the kinase activity in the presence of these inhibitors using the peptide GS-2 as substrate, a serine-phosphorylated small peptide recognized by the enzyme as primed substrate. Kinetic experiments were performed by varying the concentrations of both GS-2 (from 15.5 to 100 μM) and inhibitors VP0.7 (5 and 10 μM), while the ATP concentration was kept constant (1 μM). Double-reciprocal plotting of the data (Figure 8C) suggests that VP0.7 acts also as noncompetitive inhibitor of GS-2 binding. These data point to VP0.7 as an interesting hit compound that may bind to an allosteric GSK-3 binding site.[37] Further medicinal chemistry work is ongoing to optimize the efficacy and the druglike properties of this promising hit compound.

In the case of human GSK-3, several tridimensional structures are present in the PDB, which allow us to see the conformational richness of this protein. To take into account such conformational richness in docking studies ("ensemble docking"), the 25 structures present in the PDB were aligned with the help of maxcluster[38] in order to find clusters corresponding to different conformations according to the global root-mean-square deviation. The global rmsd did not give any clue about what structures should be selected for docking purposes, as it can be appreciated in Figure 9.

The rmsd ranges 0.2–1.8 Å, with the maximum difference corresponding to 1GNG vs 2O5K. Excluding this case, no clear differences among tridimensional structures can be appreciated according to the backbone's rmsd. However, a visual inspection of all structures shows clear differences in the "P-loop" which determines the activation state of this enzyme, although such differences become smeared when the global rmsd is taken into account, as they correspond to small protein fragments. Finally, three structures were selected according to the "P-loop" conformation: 1PYX, 1Q41, and 1Q4L.

In order to find the preferential binding site of compound VP0.7 and to see if it matches with any of fpocket's results, we have performed the docking studies considering the whole protein surface. To this end, the compound was docked in each of the above-mentioned structures (see Experimental Section) with Autodock software and the best docking clusters for each structure provided by Autodock (not located in the ATP and substrate binding site either) were considered for further analysis. In all cases, the predicted binding site matches with pocket no. 7 reported by fpocket with highly similar binding modes (Figure 10). Among these three solutions, the cluster

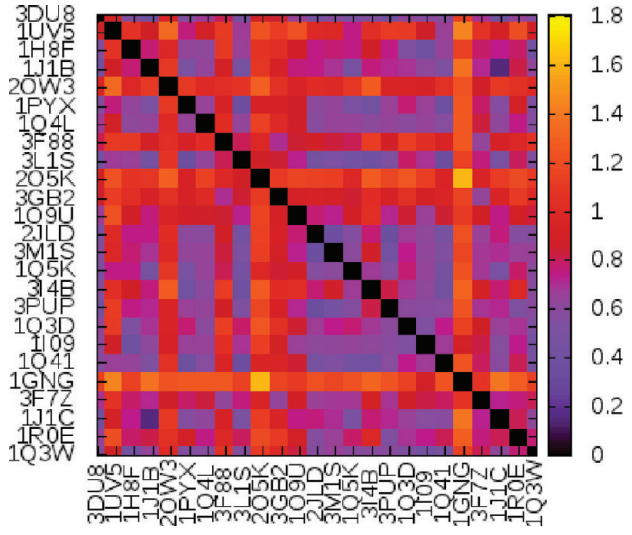

Figure 9. rmsd matrix (in angstroms) of the backbone (N, C, O, C_α, C_β) for the 25 GSK3 structures present in the protein data bank.

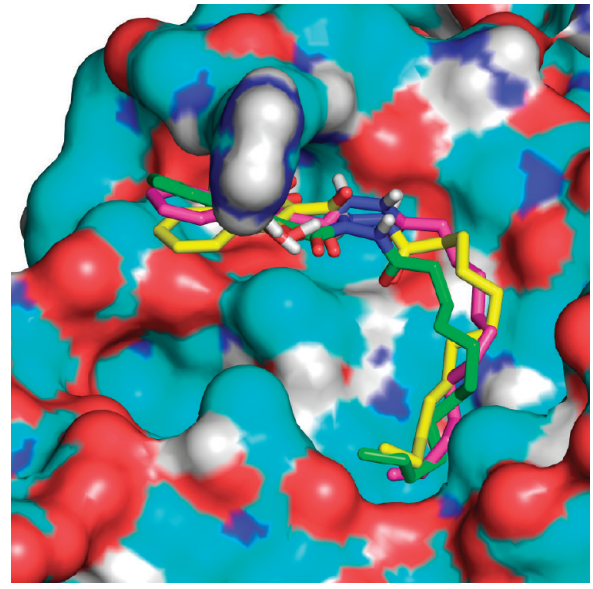

Figure 10. Superposition of the 1PYX crystal structure and the best docking solutions found for structures 1PYX (green), 1Q41 (yellow), and 1Q4L (magenta), respectively.

with the best energy was found for structure 1PYX, for which the resulting protein–ligand complex was minimized with the MMFF94 force field for the final analysis.

In the resulting structure, the inhibitor VP0.7 is located in pocket 7 with the aromatic ring sandwiched between residues Arg209 and Thr235. In this orientation, it has the benefit of a cation–π interaction with Arg209 and a hydrophobic interaction with Thr235's methyl group. Furthermore, a hydrogen bond is established between the oxygen of the inhibitor and the Ser236's backbone NH group (d = 2.4 Å). Finally, the inhibitor's aliphatic chain is extended around the hydrophobic region determined by residues Leu169, Pro331, and Thr330 (see Figure 11).

In order to provide an hypothesis for the allosteric mechanism of VP0.7, the original structure of 1PYX was compared to the final docking complex (see Figure 12). A couple of clear effects can be appreciated involving residues of

dx.doi.org/10.1021/jm200996g | J. Med. Chem. 2011, 54, 8461–8470

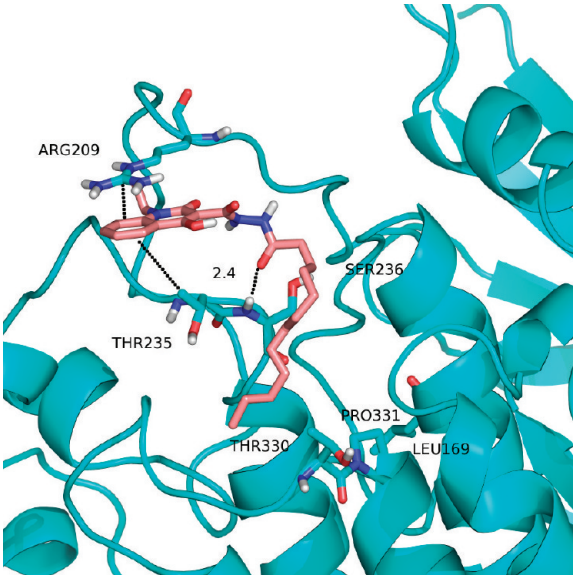

Figure 11. Suggested binding mode for compound VP0.7 in pocket no. 7 (structure 1PYX).

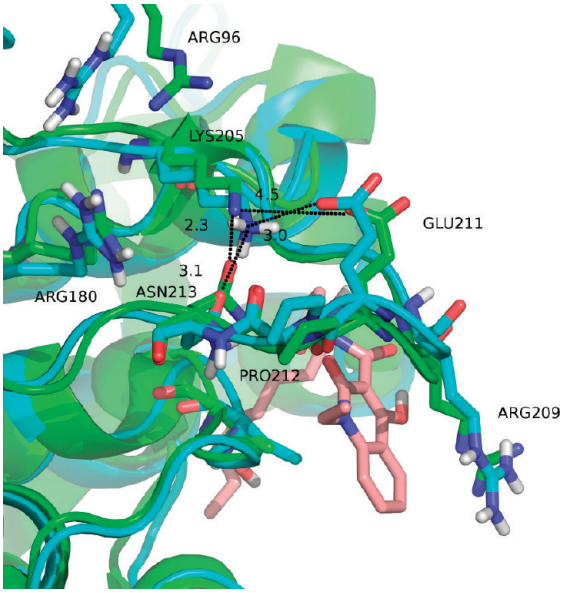

Figure 12. Local enzyme distortion upon VP0.7 binding in structure 1PYX, before binding (green) and after ligand−complex minimization (cyan).

the substrate binding site. The distance between Lys205's NZ and Glu211's OE1 is greatly reduced to 1.5 Å. At the same time, the distance between Lys205's NZ and Asn213's OD1 becomes increased to 0.7 Å, leading to an "A-loop" mobility restriction which could affect substrate binding. A conformational change on the GSK-3 substrate binding site after the binding of VP0.7 to the enzyme is observed in these calculations.

The previously described calculated binding mode for VP0.7 is in complete agreement with the experimental data obtained and provides one of the first small molecule allosteric inhibitors of GSK-3. These results are being considered in further hit-to-lead optimization steps currently in process.

CONCLUSIONS

In the present study we have analyzed the enzyme GSK-3 with fpocket and hpocket programs, designed to find druggable cavities in protein surfaces. Seven different pockets, well conserved on the surface of the 25 different GSK-3 structures used in this study, have been found. Three of these cavities turned out to be the known binding sites of GSK-3, where the ATP, the substrate, and the peptides axin/fratide bind to this protein.

We have also discovered four new druggable cavities on GSK-3 in which different ligands could interact. One of them is situated on the C-terminal lobe of the kinase, and it is very exposed to solvent. Another is located in the hinge region between the C- and N-terminal lobes. And finally, two of them are situated on the N-lobe of GSK-3. The binding therein of the recently discovered quinoline derivative VP0.7, a non-ATP nor substrate competitive GSK-3 inhibitor, is here proposed. Docking studies proposed a change in the activation loop of the enzyme that may be responsible for this allosteric modulation.

In summary, we have mapped the GSK-3 surface, discovering four potential allosteric sites that should be used for future rational drug design and discovery of small selective inhibitors that may reach clinical development as future therapies for severe unmet diseases where GSK-3 is up-regulated.

EXPERIMENTAL SECTION

Molecular Modeling. *Cavity Detection.* In order to determine different cavities on the GSK-3 enzyme, the Fpocket software, a highly scalable and free open source pocket detection software package, was used. Fpocket is freely available for download at http://www.sourceforge.net/projects/fpocket.[29] As input, fpocket software used simple standard Protein Data Bank files, which were obtained from the PDB webpage (www.pdb.org). All the available GSK-3 structures (1GNG, 1H8F, 1I09, 1J1B, 1J1C, 1O9U, 1PYX, 1Q3D, 1Q3W, 1Q41, 1Q4L, 1Q5K, 1R0E, 1UV45, 2JLD, 2O5K, 2OW3, 3DU8, 3F7Z, 3F88, 3GB2, 3I4B, 3L1S, 3M1S, 3PUP) were taken. Water molecules, ligands, and metal ions were removed previously to the fpocket analysis using the Pymol program (www.Pymol.org). On program termination, every query structure with embedded centers of pocket α-spheres was analyzed by visual inspection. After all structures were studied, the principal pockets were organized as shown in Table 2, taking into account the scores given by the fpocket program. These results were confirmed by employing the hpocket application from the fpocket package. With hpocket, homologous structures were identified from GSK-3 structures. Sequence-based identification was performed using CS-Blast[39] on the PDB,[40] filtering the hits in terms of e-value, coverage, identity, and maximal number. Structure-based identification makes use of the Astral/SCOP[41] classification, using the family level. The hits were then superimposed using an ancillary facility based on TM-align.[42]

Pocket Validation. Discovered pockets were validated using known crystal structures of some ligands bound to them. For the ATP binding site, we have used the complex with allsterpaullone (1Q3W) and AR-A014418 (1Q5K). The substrate binding site has been validated using the complex with hepes (1H8F), and finally, the complex with fratide (1GNG) was used to validate the binding site of Axin/fratide peptides. Crystal structures of these different ligands were superimposed to the fpockets results.

Docking Studies. To take into account the conformational richness of GSK-3 in docking studies ("ensemble docking"), three different structures were selected according to the "P-loop" conformation, which mostly determines the "activation" state of the enzyme: 1PYX, 1Q41, and 1Q4L. Before docking calculations, ligands, metals, waters, and cocrystallized phosphates were removed. The resulting structures were set up with the help of Sybyl 8.0[41] software by adding hydrogens,

capping n- and c-terminal residues, and removing clashes and amide bumps. The docking studies were made using Autodock1.5.4 rev30[43] software. On the other hand, the structure of compound VP0.7 was set up with Sybyl8.0 and finally minimized with the MMFF94 force field until a 0.01 kcal/mol gradient was reached. Finally, a grid of points covering the whole enzyme was computed for each structure. In docking experiments, a Lamarckian genetic algorithm was chosen and default parameters were used except "Number of GA runs", "Population size", and "Maximum number of evals", which were set to 100, 100, and 3×10^6, respectively.

The final best docking clusters (within the default 2.0 Å rmsd) according to the binding energies and relative population provided by Autodock were analyzed by visual inspection in each selected structure. Docking solutions in ATP or substrate binding sites for VP0.7 were not considered according to experimental kinetic studies. Attention was paid only in docking binding sites matching the most frequent sites reported by fpocket. Finally, the selected ligand–receptor binding modes were processed by adding hydrogens and minimized with the MMFF94 force field implemented on Sybyl 8.0 until a gradient of 0.01 kcal·mol^{-1} was reached.

Biology. *Compounds.* Manzamine A was kindly provided by Prof. M. T. Hamman. *N*′-Dodecanoyl-1-ethyl-4-hydroxy-2-oxo-1,2-dihydroquinoline-3-carbohydrazide (VP0.7) was prepared according patent application no. P201131582. All compounds were tested for purity before biological evaluation, being >95% pure by HPLC analyses.

Inhibition of GSK-3β. Human recombinant GSK-3β was purchased from Millipore (Millipore Iberica S.A.U.) The prephosphorylated polypeptide substrate was purchased from Millipore (Millipore Iberica S.A.U.). Kinase-Glo Luminescent Kinase Assay was obtained from Promega (Promega Biotech Ibérica, SL). ATP and all other reagents were from Sigma-Aldrich (St. Louis, MO). Assay buffer contained 50 mM HEPES (pH 7.5), 1 mM EDTA, 1 mM EGTA, and 15 mM magnesium acetate.

The method of Baki et al.[44] was followed for the inhibition of GSK-3β. Kinase-Glo assays were performed in assay buffer using black 96-well plates. In a typical assay, 10 μL (10 μM) of test compound (dissolved in dimethyl sulfoxide [DMSO] at 1 mM concentration and diluted in advance in assay buffer to the desired concentration) and 10 μL (20 ng) of enzyme were added to each well followed by 20 μL of assay buffer containing 25 μM substrate and 1 μM ATP. The final DMSO concentration in the reaction mixture did not exceed 1%. After 30 min of incubation at 30 °C, the enzymatic reaction was stopped with 40 μL of Kinase-Glo reagent. Glow-type luminescence was recorded after 10 min using a FLUOstar Optima (BMG Labtechnologies GmbH, Offenburg, Germany) multimode reader. The activity is proportional to the difference of the total and consumed ATP. The inhibitory activities were calculated on the basis of maximal activities measured in the absence of inhibitor. The IC_{50} was defined as the concentration of each compound that reduces 50% the enzymatic activity with respect to that without inhibitors.

GSK-3 Reversibility Studies. To study the type of enzymatic inhibition for the new compound, assays were performed to determine the activity of the enzyme after several times of incubation of the enzyme with the inhibitor. A reversible inhibitor does not increase the inhibition of the enzyme with the time of incubation, while an irreversible inhibitor increases the inhibition percentage as it increases the time of incubation with the enzyme.

Kinetic Studies on GSK-3β. To investigate the inhibitory mechanism of manzamide and VP0.7 on GSK-3β, several kinetic experiments were performed. Lineweaver–Burk plots of enzyme kinetics are shown in Figures 6 and 8.

Kinetic experiments varying both GS-2 (from 12.5 to 100 μM) and manzamine (from 5 to 10 μM) concentrations were performed. Double-reciprocal plotting of the data is depicted in Figure 6.

Kinetic experiments varying both ATP (from 1 to 50 μM) and VP0.7 (from 5 to 10 μM) concentrations were performed using the ADP-Glo Kinase Assay.[45] We have also studied the substrate dependence of the kinase activity in the presence of VP0.7 using the peptide GS-2 as substrate. Kinetic experiments were performed varying the concentrations of both GS-2 (from 15.5 to 100 μM) and VP0.7 (5 and 10 μM), while the ATP concentration was kept constant (1 μM). Double-reciprocal plotting of the data is depicted in Figure 9.

AUTHOR INFORMATION

Corresponding Author

*Telephone: +34915680010. E-mail: amartinez@iqm.csic.es.

Author Contributions

†These authors contributed equally to the manuscript

ACKNOWLEDGMENTS

The authors gratefully acknowledge the financial support of Ministry of Science and Innovation (MICINN, project no. SAF2009-13015-C02-01) and Instituto de Salud Carlos III (ISCiii, project no. RD07/0060/0015). V.P. and D.I.P. acknowledge pre- and postdoctoral fellowships, respectively, from CSIC (JAE program). Mark T. Hamann is kindly acknowledged for providing a small sample of manzamine A.

ABBREVIATIONS USED

GSK-3, glycogen synthase kinase 3; AD, Alzheimer's disease; TDZD, thiadiazolidindione; HMK, halomethylketone; PDB, Protein Data Bank

REFERENCES

(1) Kannoji, A.; Phukan, S.; Sudher Babu, V.; Balaji, V. N. GSK3beta: a master switch and a promising target. *Expert Opin. Ther. Targets* **2008**, *12*, 1443–1455.

(2) In *Glycogen synthase kinase 3 (GSK-3) and its inhibitors*; Martinez, A., Castro, A., Medina, M., Eds.; John Wiley & Sons: Hoboken, NJ, 2006.

(3) Martinez, A. Preclinical efficacy on GSK-3 inhibitors: Towards a future generation of powerful drugs. *Med. Res. Rev.* **2008**, *28*, 773–796.

(4) Hooper, C.; Killick, R.; Lovestone, S. The GSK3 hypothesis of Alzheimer's disease. *J. Neurochem.* **2008**, *104*, 1433–1439.

(5) del Ser, T. Phase IIa clinical trial on Alzheimer's disease with NP12, a GSK-3 inhibitor. *Alzheimer's Dementia* **2010**, *6*, S147.

(6) Martinez, A.; Perez, D. I. GSK-3 inhibitors: A ray of hope for the treatment of Alzheimer's disease? *J. Alzheimers Dis.* **2008**, *15*, 181–191.

(7) Chico, L. K.; Van Eldik, L. J.; Watterson, D. M. Targeting protein kinases in central nervous system disorders. *Nat. Rev. Drug Discovery* **2009**, *8*, 892–909.

(8) Cohen, P.; Goedert, M. GSK3 inhibitors: Development and therapeutic potential. *Nat. Rev. Drug Discovery* **2004**, *3*, 479–487.

(9) Martinez, A.; Castro, A.; Dorronsoro, I.; Alonso, M. Glycogen synthase kinase 3 (GSK-3) inhibitors as new promising drugs for diabetes, neurodegeneration, cancer, and inflammation. *Med. Res. Rev.* **2002**, *22*, 373–384.

(10) Eglen, R. M.; Reisine, T. The current status of drug discovery against the human kinome. *Assay Drug Dev. Technol.* **2009**, *7*, 22–43.

(11) Eglen, R.; Reisine, T. Drug discovery and the human kinome: Recent trends. *Pharmacol. Ther.* **2011**, *130*, 144–156.

(12) McInnes, C.; Fischer, P. M. Strategies for the design of potent and selective kinase inhibitors. *Curr. Pharm. Des.* **2005**, *11*, 1845–1863.

(13) Martinez, A.; Gil, C.; Perez, D. I. Glycogen synthase kinase 3 inhibitors in the next horizon for Alzheimer's disease treatment. *Int. J. Alzheimer's Dis.* **2011**, *2011*, 280502.

(14) Martinez, A.; Alonso, M.; Castro, A.; Perez, C.; Moreno, F. J. First non-ATP competitive glycogen synthase kinase 3 beta (GSK-3beta) inhibitors: Thiadiazolidinones (TDZD) as potential drugs for the treatment of Alzheimer's disease. *J. Med. Chem.* **2002**, *45*, 1292–1299.

(15) Mazanetz, M. P.; Fischer, P. M. Untangling tau hyperphosphorylation in drug design for neurodegenerative diseases. *Nat. Rev. Drug Discovery* **2007**, *6*, 464−479.
(16) Conde, S.; Perez, D. I.; Martinez, A.; Perez, C.; Moreno, F. J. Thienyl and phenyl alpha-halomethyl ketones: New inhibitors of glycogen synthase kinase (GSK-3beta) from a library of compound searching. *J. Med. Chem.* **2003**, *46*, 4631−4633.
(17) Perez, D. I.; Conde, S.; Perez, C.; Gil, C.; Simon, D.; Wandosell, F.; Moreno, F. J.; Gelpi, J. L.; Luque, F. J.; Martinez, A. Thienylhalomethylketones: Irreversible glycogen synthase kinase 3 inhibitors as useful pharmacological tools. *Bioorg. Med. Chem.* **2009**, *17*, 6914−6925.
(18) Perez, D. I.; Palomo, V.; Perez, C.; Gil, C.; Dans, P. D.; Luque, F. J.; Conde, S.; Martinez, A. Switching reversibility to irreversibility in glycogen synthase kinase 3 inhibitors: Clues for specific design of new compounds. *J. Med. Chem.* **2011**, 4042−4056.
(19) Eldar-Finkelman, H.; Eisenstein, M. Peptide inhibitors targeting protein kinases. *Curr. Pharm. Des.* **2009**, *15*, 2463−2470.
(20) Fraser, E.; Young, N.; Dajani, R.; Franca-Koh, J.; Ryves, J.; Williams, R. S.; Yeo, M.; Webster, M. T.; Richardson, C.; Smalley, M. J.; Pearl, L. H.; Harwood, A.; Dale, T. C. Identification of the Axin and Frat binding region of glycogen synthase kinase-3. *J. Biol. Chem.* **2002**, *277*, 2176−2185.
(21) Eldar-Finkelman, H.; Licht-Murava, A.; Pietrokovski, S.; Eisenstein, M. Substrate competitive GSK-3 inhibitors—Strategy and implications. *Biochim. Biophys. Acta* **2010**, *1804*, 598−603.
(22) Shapira, M.; Licht, A.; Milman, A.; Pick, C. G.; Shohami, E.; Eldar-Finkelman, H. Role of glycogen synthase kinase-3 beta in early depressive behavior induced by mild traumatic brain injury. *Mol. Cell. Neurosci.* **2007**, *34*, 571−577.
(23) Hamann, M.; Alonso, D.; Martin-Aparicio, E.; Fuertes, A.; Perez-Puerto, M. J.; Castro, A.; Morales, S.; Navarro, M. L.; Del Monte-Millan, M.; Medina, M.; Pennaka, H.; Balaiah, A.; Peng, J.; Cook, J.; Wahyuono, S.; Martinez, A. Glycogen synthase kinase-3 (GSK-3) inhibitory activity and structure-activity relationship (SAR) studies of the manzamine alkaloids. Potential for Alzheimer's disease. *J. Nat. Prod.* **2007**, *70*, 1397−1405.
(24) Alonso, D.; Martinez, A. Marine compounds as a new source for glycogen synthase kinase 3 inhibitors. In *Glycogen synthase kinase 3 (GSK-3) and its inhibitors*; Martinez, A., Castro, A., Medina, M., Eds.; John Wiley & Sons: Hoboken, NJ, 2006; pp 307−331.
(25) Peng, J. N.; Kudrimoti, S.; Prasanna, S.; Odde, S.; Doerksen, R. J.; Pennaka, H. K.; Choo, Y. M.; Rao, K. V.; Tekwani, B. L.; Madgula, V.; Khan, S. I.; Wang, B.; Mayer, A. M. S.; Jacob, M. R.; Tu, L. C.; Gertsch, J.; Hamann, M. T. Structure-activity relationship and mechanism of action studies of manzamine analogues for the control of neuroinflammation and cerebral infections. *J. Med. Chem.* **2010**, *53*, 61−76.
(26) Pérot, S.; Sperandio, O.; Miteva, M. A.; Camproux, A. C.; Villoutreix, B. O. Druggable pockets and binding site centric chemical space: A paradigm shift in drug discovery. *Drug Discovery Today* **2010**, *15*, 656−667.
(27) Schmidtke, P.; Souaille, C.; Estienne, F.; Baurin, N.; Kroemer, R. T. Large-scale comparison of four binding site detection algorithms. *J. Chem. Inf. Model.* **2010**, *50*, 2191−2200.
(28) Schmidtke, P.; Barril, X. Understanding and predicting druggability. A high-throughput method for detection of drug binding sites. *J. Med. Chem.* **2010**, *53*, 5858−5867.
(29) Le Guilloux, V.; Schmidtke, P.; Tuffery, P. Fpocket: an open source platform for ligand pocket detection. *BMC Bioinf.* **2009**, *10*, 168.
(30) Schmidtke, P.; Le Guilloux, V.; Maupetit, J.; Tuffery, P. fpocket: online tools for protein ensemble pocket detection and tracking. *Nucleic Acids Res.* **2010**, *38*, W582−W589.
(31) Schultz, C.; Link, A.; Leost, M.; Zaharevitz, D. W.; Gussio, R.; Sausville, E. A.; Meijer, L.; Kunick, C. Paullones, a series of cyclin-dependent kinase inhibitors: synthesis, evaluation of CDK1/cyclin B inhibition, and in vitro antitumor activity. *J. Med. Chem.* **1999**, *42*, 2909−2919.
(32) Bhat, R.; Xue, Y.; Berg, S.; Hellberg, S.; Ormo, M.; Nilsson, Y.; Radesater, A. C.; Jerning, E.; Markgren, P. O.; Borgegard, T.; Nylof, M.; Gimenez-Cassina, A.; Hernandez, F.; Lucas, J. J.; Diaz-Nido, J.; Avila, J. Structural insights and biological effects of glycogen synthase kinase 3-specific inhibitor AR-A014418. *J. Biol. Chem.* **2003**, *278*, 45937−45945.
(33) Dajani, R.; Fraser, E.; Roe, S. M.; Young, N.; Good, V.; Dale, T. C.; Pearl, L. H. Crystal structure of glycogen synthase kinase 3 beta: Structural basis for phosphate-primed substrate specificity and autoinhibition. *Cell* **2001**, *105*, 721−732.
(34) Ibrahim, M. A.; Shilabin, A. G.; Prasanna, S.; Jacob, M.; Khan, S. I.; Doerksen, R. J.; Hamann, M. T. 2-N-Methyl modifications and SAR studies of manzamine A. *Bioorg. Med. Chem.* **2008**, *16*, 6702−6706.
(35) Osolodkin, D. I.; Shulga, D. A.; Palyulin, V. A.; Zefirov, N. S. Interaction of manzamine A with glycogen synthase kinase 3beta: a molecular dynamics study. *Russ. Chem. Bull., Int. Ed.* **2010**, *59*, 1983−1993.
(36) Licht-Murava, A.; Plotkin, B.; Eisenstein, M.; Eldar-Finkelman, H. Elucidating substrate and inhibitor binding sites on the surface of GSK-3beta and the refinement of a competitive inhibitor. *J. Mol. Biol.* **2011**, *408*, 366−378.
(37) Martinez, A.; Gil, C.; Palomo, V.; Perez, C.; Perez, D. I. *Moduladores alostericos de GSK-3 heterociclicos*. P201131582
(38) http://helix.nih.gov/Applications/maxcluster.html.
(39) Biegert, A.; Soding, J. Sequence context-specific profiles for homology searching. *Proc. Natl. Acad. Sci. U. S. A.* **2009**, *106*, 3770−3775.
(40) Berman, H. M.; Westbrook, J.; Feng, Z.; Gilliland, G.; Bhat, T. N.; Weissig, H.; Shindyalov, I. N.; Bourne, P. E. The Protein Data Bank. *Nucleic Acids Res.* **2000**, *28*, 235−242.
(41) Chandonia, J. M.; Hon, G.; Walker, N. S.; Lo Conte, L.; Koehl, P.; Levitt, M.; Brenner, S. E. The ASTRAL Compendium in 2004. *Nucleic Acids Res.* **2004**, *32*, D189−D192.
(42) Zhang, Y.; Skolnick, J. TM-align: A protein structure alignment algorithm based on the TM-score. *Nucleic Acids Res.* **2005**, *33*, 2302−2309.
(43) Morris, G. M.; Goodsell, D. S.; Halliday, R. S.; Huey, R.; Hart, W. E.; Belew, R. K.; Olson, A. J. Automated docking using a Lamarckian genetic algorithm and an empirical binding free energy function. *J. Comput. Chem.* **1998**, *19*, 1639−1662.
(44) Baki, A.; Bielik, A.; Molnar, L.; Szendrei, G.; Keseru, G. M. A high throughput luminescent assay for glycogen synthase kinase-3beta inhibitors. *Assay Drug Dev. Technol.* **2007**, *5*, 75−83.
(45) ADP-Glo Kinase Assay Technical Manual: www.promega.com/tbs/.